

PAPER • OPEN ACCESS

Multichannel single center method

To cite this article: Nikolay M Novikovskiy *et al* 2022 *J. Phys. B: At. Mol. Opt. Phys.* **55** 175001

View the [article online](#) for updates and enhancements.

You may also like

- [Identification of damage parameters of a full-scale steel structure damaged by seismic loading](#)
Edgar Görl and Michael Link
- [Optical MEMS-based micromirror arrays for active light steering in smart windows](#)
Hartmut Hillmer, Basim Al-Qargholi, Muhammad Mohsin Khan *et al.*
- [Angular emission distribution of O 1s photoelectrons of uniaxially oriented methanol](#)
L Kaiser, K Fehre, N M Novikovskiy *et al.*



IOP | ebooks™

Bringing together innovative digital publishing with leading authors from the global scientific community.

Start exploring the collection—download the first chapter of every title for free.

Multichannel single center method

Nikolay M Novikovskiy^{1,2}, Anton N Artemyev¹, Dmitrii V Rezvan¹,
Boris M Lagutin³ and Philipp V Demekhin^{1,*} 

¹ Institut für Physik und CINSaT, Universität Kassel, Heinrich-Plett-Str. 40, 34132 Kassel, Germany

² Institute of Physics, Southern Federal University, 344090 Rostov-on-Don, Russia

³ Rostov State Transport University, 344038 Rostov-on-Don, Russia

E-mail: demekhin@physik.uni-kassel.de

Received 15 May 2022, revised 4 July 2022

Accepted for publication 7 July 2022

Published 10 August 2022



Abstract

A multichannel single center (MCSC) method for the theoretical description of the electron continuum spectrum in molecules is reported. The method includes coupling between different continuum channels via electron correlations and describes, thereby, photoelectron continuum in the Tamm–Dancoff (configuration interaction singles) approximation. Basic equations of the non-iterative one-channel single center (SC) method and their extension to the MCSC method are presented, and an efficient scheme for their numerical solution is outlined. The method is tested on known illustrative examples of the Ar 3s⁻, HCl 4σ⁻ and N₂ 1σ⁻ photoionization processes, where inter-channel coupling plays a very important role. Unlike our previous SC studies, the present MCSC method can be reliably applied to photoionization of outer and valence molecular orbitals, where inter-channel correlations in the continuum might be relevant.

Keywords: computational and mathematical techniques in atomic and molecular physics, photon interactions with molecules, photoionization and photodetachment

(Some figures may appear in colour only in the online journal)

1. Introduction


Theoretical description of the electron continuum spectrum in molecules is a nontrivial task, which is difficult to solve with standard quantum chemistry methods implementing basis orbitals localized on atomic centers. Therefore, in the last decades, many comprehensive theoretical and computational approaches to solve the electron-continuum problem in molecules were developed. Just to mention a few currently used methods: Stieltjes imaging techniques [1–4]; different scattering [5–8], multichannel Schwinger [9–12], and R-matrix [13–17] methods; random phase approximation with exchange (RPAE) for diatomic molecules [18–22]; density functional theory [23, 24] (DFT) or time-dependent density functional theory [25–29] (TDDFT) B-spline LCAO formalisms; continuum multiple scattering method (CMS-X α)

with local exchange correlation [30–32]; single center (SC) method [33–38]; and other approaches.

Some of the available methods [5–8, 30–37] describe the electron continuum in one-channel approximation, where the photoelectron leaves a system in the well-defined ionic state. Thereby, correlations of the photoelectron with electrons in the ionic core are neglected. A prominent example of such correlations is the so-called inter-channel interaction, where two continuum channels are coupled via an electron–electron interaction. A physical picture behind this effect is as follows: a photoelectron emitted from one bound orbital knocks-out electron from another bound orbital being itself recaptured to the original one. In many cases, it is impossible to satisfactorily describe a near-threshold region of the photoionization cross section without accounting for the inter-channel interaction [39, 40].

In the photoionization of atoms, importance of the inter-channel coupling was first predicted theoretically [41, 42] and then verified experimentally [43–46]. It resulted in a near-threshold correlation minimum in the 3s-photoionization cross

* Author to whom any correspondence should be addressed.

 Original content from this work may be used under the terms of the [Creative Commons Attribution 4.0 licence](https://creativecommons.org/licenses/by/4.0/). Any further distribution of this work must maintain attribution to the author(s) and the title of the work, journal citation and DOI.

section of Ar, which emerges owing to the inter-channel coupling between the 3s- and 3p-photoionization channels [13, 41, 42, 47]. Similar effect of the inter-channel coupling (between the 4σ-, 5σ-, and 2π-photoionization continua) was also found in the 4σ-photoionization of HCl molecule [48, 49]. The effect is present not only in the outer-shell photoionization, but also in the inner-shell photoionization of molecules [19, 20]. As predicted in those works, coupling between the 1σ_gεσ_u and 1σ_uεσ_g channels shares a near-threshold shape-resonance between the two partial channels, while without coupling it is present only in the 1σ_gεσ_u channel.

The methods which enable accounting for the inter-channel correlations can be conveniently grouped in two classes. The post-coupling methods, such as, e.g., different realizations of the RPAE [18–22, 50–53] or K-matrix theory [53–55], couple photoelectron continua obtained in the one-channel approximation. On the contrary, the pre-coupling methods, such as, e.g., multichannel Schwinger [9–12] and R-matrix [13–16] methods, or different realizations of the multichannel multi-configuration interaction methods [56–58], focus on the direct calculation of the multichannel photoelectron continuum wave functions. However, most of those methods are restricted to the theoretical description of the photoelectron continuum in atoms, and less [9–16, 18–22] in molecules.

The present work reports on further developments of the SC method [33–37], which was among the first methods for the electron continuum calculations in molecules [33]. The method represents one-particle molecular orbitals by expansions over spherical functions with respect to a single molecular center. Traditional way of its realization is to represent partial waves via a fixed radial basis and use a variational principle to minimize the total energy of an electronic state [34, 49, 59–64]. However, for photoelectron in the continuum, it is more efficient to solve an inhomogeneous system of coupled Hartree–Fock equations for the radial partial waves [35, 65–70]. In the last two decades, our version of the single center method [34, 49, 59–64] was considerably improved by incorporating a non-iterative scheme to account for the non-local exchange interaction [71, 72] and implementing an efficient procedure for the numerical solution of the system of coupled differential equations in diatomic [36] and polyatomic [37] molecules on a radial grid. Simultaneously, a time-dependent formulation [73–75] of the SC method was developed.

Because partial photoelectron waves in the continuum are sought in the SC method as the solutions with given angular momentum and its projection, the method is particularly suited for studying the angular-resolved photoionization and decay spectra of molecules. We successfully applied our SC method to study laboratory-frame [37, 76–87] and also molecular-frame [88–100] angular emission distributions of photoelectrons in molecules. However, in its present realization, the SC method describes photoelectron continuum in the one-channel Hartree–Fock approximation. In the present work, we develop multichannel version of our single center method (MCSC). To this end, we first summarize in section 2 basic equations of the non-iterative one-channel SC method. Thereafter, in section 3, we formulate its multichannel extension. Finally, we consider three applications of the MCSC method to photoionization of

atoms and molecules (section 4). We conclude in section 5 with a brief summary.

2. Non-iterative single center method

Below, we outline the one-channel SC method. According to the method, the spatial part of the one-particle molecular orbital with a kinetic energy ε is represented with respect to a molecular center as an expansion over spherical harmonics Y_{ℓm} with a given projection m of the angular momentum ℓ on the quantization z-axis [36, 37]:

$$\Psi_\varepsilon(\mathbf{r}) = \sum_{\ell m} \frac{P_{\varepsilon\ell m}(r)}{r} Y_{\ell m}(\theta, \varphi), \quad (1)$$

where {r, θ, φ} are spherical coordinates. In the one-channel approximation, the variational principle yields the following system of coupled inhomogeneous Hartree–Fock equations for the radial partial waves P_{εℓm}(r) of the photoelectron in continuum [36, 37] (atomic units are used throughout):

$$\begin{aligned} \frac{d^2 P_{\varepsilon\ell m}(r)}{dr^2} = & \sum_{\ell' m'} \left[\left(\frac{\ell(\ell+1)}{r^2} - 2\varepsilon \right) \delta_{\ell\ell'} \delta_{mm'} + 2V_{\ell m \ell' m'}^{\text{ne}}(r) \right. \\ & \left. + 2J_{\ell m \ell' m'}^{\text{ee}}(r) \right] P_{\varepsilon\ell' m'}(r) + \sum_c 2b_c \\ & \times \sum_{kq} \sum_{\ell'_c m'_c} (-1)^{m'_c} \sqrt{(2\ell'_c+1)(2\ell+1)} \\ & \times \begin{pmatrix} \ell'_c & k & \ell \\ 0 & 0 & 0 \end{pmatrix} \begin{pmatrix} \ell'_c & k & \ell \\ -m'_c & q & m \end{pmatrix} \frac{Y_{kq}(\Psi_c, \Psi_\varepsilon)}{r}, \\ & \times P_{n_c \ell'_c m'_c} \end{aligned} \quad (2)$$

with the following normalization condition for a positive photoelectron kinetic energy ε > 0:

$$\sum_{\ell m} \langle P_{\varepsilon\ell m} | P_{\varepsilon'\ell m} \rangle = \delta(\varepsilon - \varepsilon'). \quad (3)$$

In the system of equation (2), the nuclear–electron interaction potential is given as

$$\begin{aligned} V_{\ell m \ell' m'}^{\text{ne}} = & - \sum_n Z_n \sum_{kq} (-1)^m \sqrt{(2\ell+1)(2\ell'+1)} \\ & \times \begin{pmatrix} \ell & k & \ell' \\ 0 & 0 & 0 \end{pmatrix} \begin{pmatrix} \ell & k & \ell' \\ -m & q & m' \end{pmatrix} \\ & \times \sqrt{\frac{4\pi}{2k+1}} Y_{kq}^*(\theta_n, \phi_n) \frac{r_{<}^k}{r_{>}^{k+1}}, \end{aligned} \quad (4)$$

where r_< = min(r, R_n), r_> = max(r, R_n), and R_n, θ_n, φ_n are the spherical coordinates of the nucleus n with charge Z_n. The potential describing the direct electrostatic Coulomb interaction J_{ℓmℓ'm'}^{ee} between the photoelectron Ψ_ε and all electrons in the molecular orbitals Ψ_c bound to the ion reads:

$$\begin{aligned}
 J_{\ell m \ell' m'}^{ee} &= \sum_c a_c \sum_{\ell_c m_c} \sum_{\ell'_c m'_c} \sum_{kq} (-1)^{m_c+m'} \\
 &\times \sqrt{(2\ell_c+1)(2\ell'_c+1)(2\ell+1)(2\ell'+1)} \\
 &\times \begin{pmatrix} \ell_c & k & \ell'_c \\ 0 & 0 & 0 \end{pmatrix} \begin{pmatrix} \ell_c & k & \ell'_c \\ -m_c & q & m'_c \end{pmatrix} \\
 &\times \begin{pmatrix} \ell' & k & \ell \\ 0 & 0 & 0 \end{pmatrix} \begin{pmatrix} \ell' & k & \ell \\ -m' & q & m \end{pmatrix} \\
 &\times y_k(\ell_c m_c, \ell'_c m'_c). \tag{5}
 \end{aligned}$$

Here, a_c are coefficients for the direct Coulomb interactions, which are determined by the electronic configuration formed by the photoelectron and the ionic core electrons, and $y_{kq}(\ell_c m_c, \ell'_c m'_c)$ are the partial harmonics of the Coulomb potential defined as

$$y_k(\ell_c m_c, \ell'_c m'_c) = \int_0^\infty \frac{r_{<}^k}{r_{>}^{k+1}} P_{n_c \ell_c m_c}^*(r') P_{n_c \ell'_c m'_c}(r') dr' \tag{6}$$

with $r_{<} = \min(r, r')$ and $r_{>} = \max(r, r')$.

The last term on the right-hand side of equation (2) with respective coefficients b_c represents the exchange Coulomb interaction of the photoelectron and all bound electrons (the two lower lines in the equation). Because of its non-locality, the system of equation (2) is inhomogeneous, which usually implies iterative solution schemes. This term contains generalized potentials $Y_{kq}(\Psi_c, \Psi_\varepsilon)$, which represent harmonics of the multiplicity kq of the exchange interaction of the photoelectron Ψ_ε with the core electron Ψ_c and explicitly read [36]:

$$\begin{aligned}
 Y_{kq}(\Psi_c, \Psi_\varepsilon) &= \sum_{\ell_c m_c} \sum_{\ell' m'} (-1)^{m_c} \sqrt{(2\ell_c+1)(2\ell'+1)} \\
 &\times \begin{pmatrix} \ell_c & k & \ell' \\ 0 & 0 & 0 \end{pmatrix} \begin{pmatrix} \ell_c & k & \ell' \\ -m_c & q & m' \end{pmatrix} \\
 &\times r \cdot y_k(\ell_c m_c, \ell' m'). \tag{7}
 \end{aligned}$$

It is straightforward to show [71] that the generalized exchange potentials (7) satisfy the following differential equation of the second order [36]:

$$\begin{aligned}
 \frac{d^2 Y_{kq}(\Psi_c, \Psi_\varepsilon)}{dr^2} &= \frac{k(k+1)}{r^2} Y_{kq}(\Psi_c, \Psi_\varepsilon) - \frac{(2k+1)}{r} \\
 &\times \sum_{\ell_c m_c} \sum_{\ell' m'} (-1)^{m_c} \sqrt{(2\ell_c+1)(2\ell'+1)} \\
 &\times \begin{pmatrix} \ell_c & k & \ell' \\ 0 & 0 & 0 \end{pmatrix} \begin{pmatrix} \ell_c & k & \ell' \\ -m_c & q & m' \end{pmatrix} \\
 &\times P_{n_c \ell_c m_c}^* P_{\varepsilon \ell' m'}. \tag{8}
 \end{aligned}$$

One can see, that the system of equation (2) for the radial partial photoelectron waves $P_{\varepsilon \ell m}(r)$ and equation (8) for the generalized exchange potentials $Y_{kq}(\Psi_c, \Psi_\varepsilon) = Y_{ckq}(r)$ are coupled to each other. As a consequence, the combined vector solution $\bar{P}(r)$

$$\bar{P} = \begin{pmatrix} P_{\varepsilon \ell m} \\ Y_{ckq} \end{pmatrix} \tag{9}$$

satisfies the following homogeneous system of coupled differential equations of the second order:

$$\frac{d^2 \bar{P}}{dr^2} = \hat{F} \bar{P} \tag{10}$$

with the quadratic matrix

$$\hat{F} = \begin{pmatrix} F_{\ell m \ell' m'} & F_{\ell m c k q} \\ F_{c k q \ell' m'} & F_{c k q c' k' q'} \end{pmatrix}. \tag{11}$$

The matrix elements of \hat{F} are given by [36, 37]:

$$\begin{aligned}
 F_{\ell m \ell' m'} &= \left(\frac{\ell(\ell+1)}{r^2} - 2\varepsilon \right) \delta_{\ell \ell'} \delta_{m m'} \\
 &+ 2V_{\ell m \ell' m'}^{ne}(r) + 2J_{\ell m \ell' m'}^{ee}(r), \tag{12a}
 \end{aligned}$$

$$\begin{aligned}
 F_{\ell m c k q} &= \frac{2b_c}{r} \sum_{\ell'_c m'_c} (-1)^{m'_c} \sqrt{(2\ell'_c+1)(2\ell+1)} \\
 &\times \begin{pmatrix} \ell'_c & k & \ell \\ 0 & 0 & 0 \end{pmatrix} \begin{pmatrix} \ell'_c & k & \ell \\ -m'_c & q & m \end{pmatrix} P_{n_c \ell'_c m'_c}, \tag{12b}
 \end{aligned}$$

$$\begin{aligned}
 F_{c k q \ell' m'} &= -\frac{(2k+1)}{r} \sum_{\ell_c m_c} (-1)^{m_c} \sqrt{(2\ell_c+1)(2\ell'+1)} \\
 &\times \begin{pmatrix} \ell_c & k & \ell' \\ 0 & 0 & 0 \end{pmatrix} \begin{pmatrix} \ell_c & k & \ell' \\ -m_c & q & m' \end{pmatrix} P_{n_c \ell_c m_c}^*, \tag{12c}
 \end{aligned}$$

$$F_{c k q c' k' q'} = \frac{k(k+1)}{r^2} \delta_{c c'} \delta_{k k'} \delta_{q q'}. \tag{12d}$$

The homogeneous system of equation (10) can be solved non-iteratively. An efficient scheme for the numerical solution of this system, implemented in our in-house computer code for the stationary SC method [36, 37] to search for mutually-orthogonal energy-normalized partial photoelectron waves, is outlined in the appendix A.

3. Multichannel single center method

We now go beyond the one-channel HF approximation for the photoelectron in continuum and introduce the MCSC method. Let us, for simplicity, consider an electronic configuration of a molecule with two doubly-occupied molecular orbitals $a^2 b^2$ (extension of the theory to more coupled channels is straightforward). Both orbitals can be ionized, creating at a given total energy two continuum channels of similar symmetries and multiplicities:

$$\begin{cases} \Psi^{(b\varepsilon)} = |a^2 b^1 \varepsilon\rangle, \\ \Psi^{(a\varepsilon')} = |a^1 b^2 \varepsilon'\rangle. \end{cases} \tag{13}$$

It is straightforward to show that these continuum channels are coupled via the following electron–electron Coulomb interaction matrix element

$$\begin{aligned} & \langle \Psi^{(b\varepsilon)} | \hat{H}^{ee} | \Psi^{(a\varepsilon')} \rangle \\ &= c^{\text{dir}} \left\langle a\varepsilon \left| \frac{1}{r_{12}} \right| b\varepsilon' \right\rangle + c^{\text{exch}} \left\langle a\varepsilon \left| \frac{1}{r_{12}} \right| \varepsilon'b \right\rangle, \end{aligned} \quad (14)$$

where, in the closed-shell case, the coefficient in front of the direct contribution is equal to $c^{\text{dir}} = -1$ for both, singlet and triplet multiplicities of the channels, and that for the exchange contribution $c^{\text{exch}} = 2$ for the singlet or $c^{\text{exch}} = 0$ for the triplet multiplicities.

Applying the variational principle, one can derive coupled differential equations for the unified vector solution (9) of each channel in (13). Those solutions are designated below as $\bar{\mathbf{P}}^{(b\varepsilon)}$ and $\bar{\mathbf{P}}^{(a\varepsilon')}$. For each channel, this system resembles equation (10) from the one-channel SC method. However, because of the inter-channel interaction (14), the two systems of equations are coupled to each other by the direct and exchange contributions. If one combines the solutions for two channels in a single vector

$$\bar{\mathbf{P}} = \begin{pmatrix} \bar{\mathbf{P}}^{(b\varepsilon)} \\ \bar{\mathbf{P}}^{(a\varepsilon')} \end{pmatrix}, \quad (15)$$

one arrives at the system of coupled homogeneous differential equations of the second order, which is similar to that solved in the one-channel SC method (equation (10)):

$$\frac{d^2 \bar{\mathbf{P}}}{dr^2} = \hat{\mathbf{F}} \bar{\mathbf{P}}. \quad (16)$$

The respective quadratic matrix $\hat{\mathbf{F}}$ can be constructed from the one-particle matrixes $\hat{F}^{(b\varepsilon)}$ and $\hat{F}^{(a\varepsilon')}$ of the two independent channels as follows

$$\hat{\mathbf{F}} = \begin{pmatrix} \{ \hat{F}^{(b\varepsilon)} \} & F_{\ell m \ell' m'}^{(b\varepsilon a\varepsilon')} & F_{\ell m k q}^{(b\varepsilon a\varepsilon')} \\ F_{\ell m \ell' m'}^{(a\varepsilon' b\varepsilon)} & F_{\ell m k q}^{(a\varepsilon' b\varepsilon)} & \{ \hat{F}^{(a\varepsilon')} \} \\ 0 & 0 & 0 \end{pmatrix}. \quad (17)$$

The matrix elements of the one-channel matrixes $\hat{F}^{(b\varepsilon)}$ and $\hat{F}^{(a\varepsilon')}$ in the diagonal of $\hat{\mathbf{F}}$ are defined in equations (11)–(12d). The non-diagonal matrix elements represent the direct $F_{\ell m \ell' m'}^{(b\varepsilon a\varepsilon')}$ and $F_{\ell m \ell' m'}^{(a\varepsilon' b\varepsilon)}$, as well as exchange $F_{\ell m k q}^{(b\varepsilon a\varepsilon')}$ and $F_{\ell m k q}^{(a\varepsilon' b\varepsilon)}$ contributions of the inter-channel coupling (14). Their explicit expressions read:

$$\begin{aligned} F_{\ell m \ell' m'}^{(b\varepsilon a\varepsilon')} &= 2c^{\text{dir}} \sum_{\ell_a m_a} \sum_{\ell'_b m'_b} \sum_{kq} (-1)^{m_a + m'} \\ &\times \sqrt{(2\ell + 1)(2\ell' + 1)(2\ell_a + 1)(2\ell'_b + 1)} \\ &\times \begin{pmatrix} \ell_a & k & \ell'_b \\ 0 & 0 & 0 \end{pmatrix} \begin{pmatrix} \ell_a & k & \ell'_b \\ -m_a & q & m'_b \end{pmatrix} \\ &\times \begin{pmatrix} \ell' & k & \ell \\ 0 & 0 & 0 \end{pmatrix} \begin{pmatrix} \ell' & k & \ell \\ -m' & q & m \end{pmatrix} \\ &\times y_k(\ell_a m_a, \ell'_b m'_b), \end{aligned} \quad (18a)$$

$$\begin{aligned} F_{\ell m \ell' m'}^{(a\varepsilon' b\varepsilon)} &= 2c^{\text{dir}} \sum_{\ell_b m_b} \sum_{\ell'_a m'_a} \sum_{kq} (-1)^{m_b + m'} \\ &\times \sqrt{(2\ell + 1)(2\ell' + 1)(2\ell_b + 1)(2\ell'_a + 1)} \\ &\times \begin{pmatrix} \ell_b & k & \ell'_a \\ 0 & 0 & 0 \end{pmatrix} \begin{pmatrix} \ell_b & k & \ell'_a \\ -m_b & q & m'_a \end{pmatrix} \\ &\times \begin{pmatrix} \ell' & k & \ell \\ 0 & 0 & 0 \end{pmatrix} \begin{pmatrix} \ell' & k & \ell \\ -m' & q & m \end{pmatrix} \\ &\times y_k(\ell_b m_b, \ell'_a m'_a), \end{aligned} \quad (18b)$$

$$\begin{aligned} F_{\ell m k q}^{(b\varepsilon a\varepsilon')} &= \frac{2c^{\text{exch}}}{r} \sum_{\ell'_b m'_b} (-1)^{m'_b} \sqrt{(2\ell + 1)(2\ell'_b + 1)} \\ &\times \begin{pmatrix} \ell'_b & k & \ell \\ 0 & 0 & 0 \end{pmatrix} \begin{pmatrix} \ell'_b & k & \ell \\ -m'_b & q & m \end{pmatrix} P_{n_b \ell'_b m'_b}, \end{aligned} \quad (18c)$$

$$\begin{aligned} F_{\ell m k q}^{(a\varepsilon' b\varepsilon)} &= \frac{2c^{\text{exch}}}{r} \sum_{\ell'_a m'_a} (-1)^{m'_a} \sqrt{(2\ell + 1)(2\ell'_a + 1)} \\ &\times \begin{pmatrix} \ell'_a & k & \ell \\ 0 & 0 & 0 \end{pmatrix} \begin{pmatrix} \ell'_a & k & \ell \\ -m'_a & q & m \end{pmatrix} P_{n_a \ell'_a m'_a}. \end{aligned} \quad (18d)$$

It should be noted, that the exchange interactions (18c) and (18d) couple partial photoelectron waves from each channel only with the generalized exchange potentials representing the respective core orbitals ionized in the opposite channel. The unified system of equation (16) can now be solved by the same numerical procedure as outlined in the appendix A.

4. Applications

As mentioned in the introduction, 3s-photoionization of Ar atom is the first example of a manifestation of the inter-channel correlations in atomic photoionization [41, 42]. It is, therefore, appropriate to test the MCSC method on this example. The present calculations included the inter-channel coupling between the 3s- and 3p-photoionization continua (four coupled 3s-, 3p_x-, 3p_y-, and 3p_z-channels) and were performed in two ways. In the first set of calculations, the Ar atom was placed in the center, and the SC expansions (1) of the occupied and continuum orbitals were restricted by $\ell_c \leq 1$ and $\ell \leq 2$, respectively. In order to simulate a molecule in the second set of calculations, the atom was shifted from the coordinate origin by +0.5 a.u. along the z-axis, and the SC expansions were extended to $\ell_c \leq 99$ and $\ell \leq 29$. Both sets of the present calculations yielded equal results, which are depicted in figure 1. As one can see, the 3s-photoionization cross section of Ar, computed with accounting for the inter-channel coupling by the MCSC method (red solid curve), exhibits a correlational minimum around the photon energy of about 40 eV. This is in agreement with the previous theoretical results, obtained by the RPAE [42] and R-matrix [13] methods, and with the selected experimental results [43, 44, 46]. Note that this minimum emerges in the theoretical results at somewhat different photon energies, owing to different relative values of the 3s and 3p binding energies used in the calculations. Note also

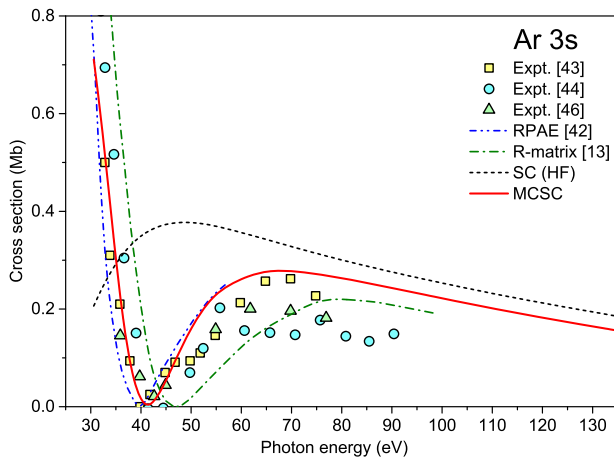


Figure 1. Theoretical and experimental Ar 3s-photoionization cross sections. Black dashed curve: Hartree–Fock, present SC calculations. Red solid curve: inter-channel coupling, present MCSC calculations. Blue dash-dot-dotted curve: RPAE calculations from reference [42]. Green dash-dotted curve: R-matrix calculations from reference [13]. The experimental partial photoionization cross section are taken from references [43, 44, 46].

that this minimum in the cross section is not present in the one-channel SC calculations, which neglect the inter-channel coupling (black dashed curve).

A similar correlational minimum exists in the 4σ -photoionization cross section of the argon-like HCl molecule [48, 49]. We, therefore, performed the respective MCSC calculations which account for the inter-channel coupling between the 4σ -, $2\pi_x$ -, $2\pi_y$ -, and 5σ -photoionization continua (analogies of the four 3s- and 3p-continua in Ar). Calculations were performed at the equilibrium internuclear distance with the Cl atom being placed in the coordinate origin. The SC expansions (1) of the occupied and continuum orbitals were restricted by $\ell_c \leq 99$ and $\ell \leq 29$. As one can see from figure 2, the inter-channel coupling results in the appearance of the correlational minimum in the 4σ -photoionization cross section of HCl around the photon energy of about 40 eV (cf, the black dashed and red solid curves, which represent the present one-channel and multichannel calculations, respectively), which is in accord with the experiment [48] and the previous calculations [49]. Quantitative disagreement between the theory and experiment can be related to a multi-reference character of the final 4σ -ionized state [49], which was neglected in the present calculations.

We, finally, considered prominent example of manifestation of the inter-channel coupling in the inner-shell photoionization of molecules [19, 20]. To this end, we studied the 1σ -photoionization of N_2 molecule (note a controversial discussion on the existence of the shape resonance in the $1\sigma_u$ -channel [101–103], which was finally confirmed in reference [104] experimentally and theoretically). The present calculations were performed in the relaxed-core approximation at the equilibrium internuclear distance of the neutral molecule. The molecular center was set in between the two nitrogen atoms, and the SC expansions of the occupied and continuum orbitals

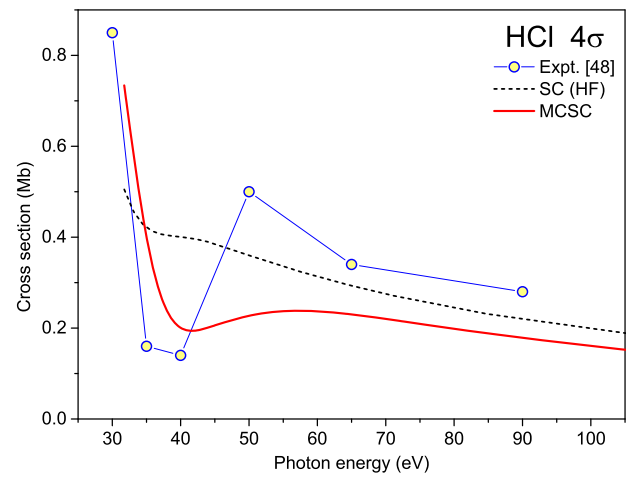


Figure 2. Theoretical and experimental HCl 4σ -photoionization cross sections. Black dashed curve: Hartree–Fock, present SC calculations. Red solid curve: inter-channel coupling, present MCSC calculations. The experimental partial photoionization cross section is taken from reference [48].

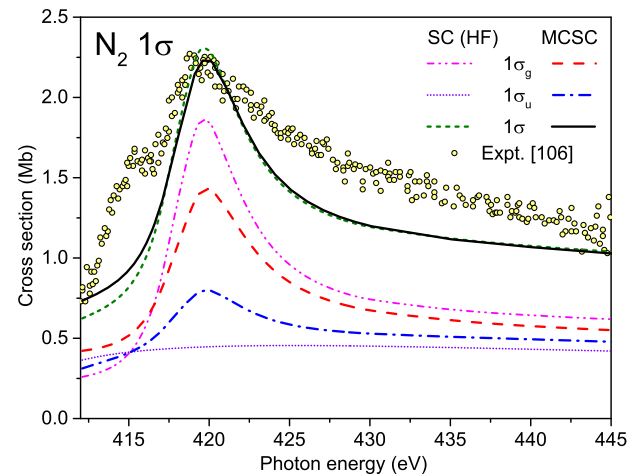


Figure 3. Partial and total N_2 1σ -photoionization cross sections. Magenta dash-dot-dotted curve: SC calculations for the partial $1\sigma_g$ -channel. Violet dotted curve: SC calculations for the partial $1\sigma_u$ -channel. Green short-dashed curve: SC calculations, 1σ total. Red dashed curve: MCSC calculations for the $1\sigma_g$ -channel. Blue dash-dotted curve: MCSC calculations for the $1\sigma_u$ -channel. Black solid curve: MCSC calculations, 1σ total. The experimental total photoionization cross section is taken from reference [105].

were restricted by $\ell_c \leq 99$ and $\ell \leq 29$. Results of the present calculations are depicted in figure 3, and they are in accord with the original predictions of references [19, 20] and also with the final results from reference [104] (see figure 2 in this reference for an overview of all available theoretical and experimental data). As one can see from figure 3 around the photon energy of about 420 eV, in the one-channel SC calculations, the shape resonance is present only in the partial $1\sigma_g$ -photoionization cross section (cf, magenta dash-dot-dotted and

violet dotted curves). After the coupling between the $1\sigma_g$ - and $1\sigma_u$ -channels is included, it emerges in both channels (cf, red dashed and blue dash-dotted curves). In the experimental total 1σ cross section [105] (circles), this shape resonance is somewhat broader than in the theory (black solid curve), which can be attributed to the effect of vibrational broadening neglected in the calculations.

5. Summary and outlook

The present work reports a further step in the development of the single center method. In its previous realization [36, 37], the method described the photoelectron continuum spectrum of molecules in the one-channel Hartree–Fock approximation. It was therefore mainly suitable to study molecular photoionization for the cases where electron correlations in the continuum are moderate and can thus be neglected. In the multichannel realization reported in this work, the MCSC method allows to couple continuum channels via the inter-channel electron–electron interaction. Thereby, an important class of correlations between the photoelectron and electrons bound in the ion can be accurately accounted for. This development significantly broadens applicability of the method to the photoionization of outer and valence molecular orbitals, for which electron correlations in the continuum may play a significant role.

Acknowledgments

The authors would like to thank Victor L Sukhorukov for many valuable discussions. NMN, ANA, DVR and PhVD acknowledge support from the Deutsche Forschungsgemeinschaft (DFG)—Project No. 492619011—DE 2366/6-1. NMN acknowledges support from the Ministry of Science and Higher Education of the Russian Federation under State Task in the field of scientific activity, Project No. 0852-2020-0032 (BAS0110/20-3-08IF). PhVD would like to thank the Rostov State Transport University for the hospitality during his research stay there, which was supported from traveling funds of the DFG Project DE 2366/1-2.

Data availability statement

The data that support the findings of this study are available upon reasonable request from the authors.

Appendix A. Numerical procedure

In order to solve the system of linear homogeneous differential equations of the second order (10), we employ a combination of the Numerov finite-difference and the vector sweep methods. The former method relates values of the unknown vector solution at three neighboring points as

$$\hat{a}_{n+1} \times \bar{P}_{n+1} - \hat{b}_n \times \bar{P}_n + \hat{a}_{n-1} \times \bar{P}_{n-1} = O(h^6), \quad (\text{A.1})$$

where matrices \hat{a} and \hat{b} are given by

$$\hat{a}_n = \left[\hat{E} - \frac{h^2}{12} \hat{F}_n \right] \quad \text{and} \quad \hat{b}_n = \left[2\hat{E} + \frac{10h^2}{12} \hat{F}_n \right]. \quad (\text{A.2})$$

Here, h is a constant integration step, and \hat{E} is a unity matrix. The latter method relates values of the unknown vector solution only at two neighboring points

$$\bar{P}_{n-1} = \hat{V}_{n-1} \times \bar{P}_n. \quad (\text{A.3})$$

Substituting this relation in equation (A.1) yields the following recurrent relation for the unknown sweep matrix \hat{V}_n :

$$\hat{V}_n = \left(\hat{b}_n - \hat{a}_{n-1} \times \hat{V}_{n-1} \right)^{-1} \times \hat{a}_{n+1}. \quad (\text{A.4})$$

Integration can be started by applying the $\hat{V}_1 = \hat{V}_2 = \hat{V}$ boundary condition for the sweep matrix at $r \rightarrow 0$, which yields

$$\hat{V} = \left(\hat{b}_2 - \hat{a}_1 \times \hat{V} \right)^{-1} \times \hat{a}_3. \quad (\text{A.5})$$

Using now equation (A.4) allows one to find the unknown sweep matrix \hat{V}_n at all radial grid points.

The linearly independent solutions of the system of equation (2) satisfy at $r \rightarrow \infty$ the following asymptotical behavior [72]:

$$P_{\ell m}^{LM}(r) = \delta_\ell^L \delta_m^M J_{\ell\ell}(r) + \mathcal{R}_{\ell m}^{LM} H_{\ell\ell}(r), \quad (\text{A.6})$$

where $J_{\ell\ell}(r)$ and $H_{\ell\ell}(r)$ are the regular and non-regular Coulomb functions [106], respectively, $\mathcal{R}_{\ell m}^{LM}$ is the reaction matrix, and indices LM enumerate linear-independent solutions, while ℓm their components. A similar condition at $r \rightarrow \infty$ for the generalized exchange potentials, which are solutions of equation (8), reads [71]:

$$Y_{ckq}(r) = \frac{B_{ckq}}{r^k}. \quad (\text{A.7})$$

We now designate unknown values of the vector solution (9) at the last grid point N (where a short-range molecular potential vanishes) as

$$\bar{P}_N^{LM} = \begin{pmatrix} \{P_{\ell m}^{LM}\}_N \\ \{Y_{ckq}^{LM}\}_N \end{pmatrix}. \quad (\text{A.8})$$

Applying the asymptotical conditions (A.6) and (A.7) together with the relation (A.3) to the last two points N and $N - 1$ of the radial grid, one can write

$$\left\{ \begin{array}{l} \bar{P}_N^{LM} - \begin{pmatrix} \mathcal{R}_{\ell m}^{LM} \{H_{\ell\ell}\}_N \\ \frac{B_{ckq}^{LM}}{r_N^k} \end{pmatrix} = \begin{pmatrix} \delta_\ell^L \delta_m^M \{J_{\ell\ell}\}_N \\ 0 \end{pmatrix} \\ \hat{V}_{N-1} \times \bar{P}_N^{LM} - \begin{pmatrix} \mathcal{R}_{\ell m}^{LM} \{H_{\ell\ell}\}_{N-1} \\ \frac{B_{ckq}^{LM}}{r_{N-1}^k} \end{pmatrix} = \begin{pmatrix} \delta_\ell^L \delta_m^M \{J_{\ell\ell}\}_{N-1} \\ 0 \end{pmatrix} \end{array} \right. \quad (\text{A.9})$$

Being solved for all solutions LM , the system of linear equation (A.9) allows one to determine the unknown values of the radial partial waves $\{P_{\varepsilon\ell m}^{LM}\}_N$ and of the generalized exchange potentials $\{Y_{ckq}^{LM}\}_N$ in the last grid point, as well as coefficients B_{ckq}^{LM} from the asymptotic relation (A.7) and the complete $\mathcal{R}_{\ell m}^{LM}$ matrix. Using now the matrix sweep relation (A.3), one can reconstruct the partial photoelectron waves in the complete radial grid. The mutually-orthogonal energy-normalized partial photoelectron waves $\mathcal{P}_{\ell m}^{LM}(r)$, which contain outgoing spherical waves only in the channel with $\ell m = LM$, can be constructed as the following linear combinations of the found solutions [54, 55]:

$$\mathcal{P}_{\ell m}^{LM} = \sum_{L'M'} (\mathcal{U}_{L'M'}^{LM})^\dagger e^{-i\eta_{L'M'}} \cos \eta_{L'M'} \sum_{L''M''} \mathcal{U}_{L''M''}^{L'M'} \mathcal{P}_{\ell m}^{L''M''}, \quad (\text{A.10})$$

where \mathcal{U} are eigenvectors of the Hermitian \mathcal{R} -matrix with real eigenvalues $-\tan \eta$.

Using the radial parts (A.10), the dipole transition amplitudes $A_{\varepsilon LMK}$ for population of the partial continuum waves with energy ε , angular momentum L , its projection M , after absorption of a photon with polarization K can now be calculated via:

$$\begin{aligned} A_{\varepsilon LMK} &= \sum_{\ell m} \sum_{\ell_c m_c} (-1)^M \sqrt{(2\ell+1)(2\ell_c+1)} \\ &\times \begin{pmatrix} \ell & 1 & \ell_c \\ 0 & 0 & 0 \end{pmatrix} \begin{pmatrix} \ell & 1 & \ell_c \\ -m & K & m_c \end{pmatrix} \\ &\times \int_0^\infty \mathcal{P}_{\ell m}^{LM}(r)^* r P_{\ell_c m_c}(r) dr. \end{aligned} \quad (\text{A.11})$$

Here, $K = 0$ represents linear and $K = \pm 1$ circular polarizations, $P_{\ell_c m_c}(r)$ are the radial parts of the single center expansion (1) of an ionized bound orbital, and the length gauge of the dipole transition operator is used explicitly. The respective transition amplitudes provide an access to different observable quantities. For intrans, the total photoionization cross section, discussed in this work, can be computed as:

$$\sigma(\varepsilon) = \frac{4\pi^2 \alpha a_0^2 \omega}{3} \sum_{LMK} |A_{\varepsilon LMK}|^2, \quad (\text{A.12})$$

where $\alpha = 1/137.036$ is the fine structure constant, the square of the Bohr radius $a_0^2 = 28.0028 \text{ Mb}$ converts the atomic units for cross sections to megabarn ($1 \text{ Mb} = 10^{-22} \text{ m}^2$), and ω is the implied photon energy.

As a final point we mention, that an accuracy of the numerical integration can be considerably improved if one introduces a new integration variable ρ , which is related to the radial variable r via [36]:

$$\rho(r) = \alpha r + \beta \ln r + \sum_n \arctan \frac{R_n - r}{\gamma_n}. \quad (\text{A.13})$$

Here, integration is performed in constant steps of ρ . The second term in equation (A.13) concentrates radial grid points in

the origin, while the third makes it symmetrically around all nuclei. Introducing a new vector solution

$$\bar{F} = \bar{P} \sqrt{\rho'_r} \quad (\text{A.14})$$

converts the system of differential equations for this solution \bar{F} to the form of equation (10) [36].

ORCID iDs

Philipp V Demekhin  <https://orcid.org/0000-0001-9797-6648>

References

- [1] Carravetta V, Ågren H, Vahtras O and Jensen H J A 2000 *J. Chem. Phys.* **113** 7790
- [2] Averbukh V and Cederbaum L S 2005 *J. Chem. Phys.* **123** 204107
- [3] Kolorenč P, Averbukh V, Gokhberg K and Cederbaum L S 2008 *J. Chem. Phys.* **129** 244102
- [4] Averbukh V et al 2011 *J. Electron Spectrosc. Relat. Phenom.* **183** 36
- [5] Zähringer K, Meyer H-D and Cederbaum L S 1992 *Phys. Rev. A* **45** 318
- [6] Zähringer K, Meyer H-D and Cederbaum L S 1992 *Phys. Rev. A* **46** 5643
- [7] Schimmelpfennig B, Nestmann B M and Peyerimhoff S D 1995 *J. Electron Spectrosc. Relat. Phenom.* **74** 173
- [8] Hjelte I et al 2005 *J. Chem. Phys.* **122** 084306
- [9] Bonhoff S, Bonhoff K, Schimmelpfennig B and Nestmann B 1997 *J. Phys. B: At. Mol. Opt. Phys.* **30** 2821
- [10] Lin P and Lucchese R R 2002 *J. Chem. Phys.* **116** 8863
- [11] Lucchese R R, Lafosse A, Brenot J C, Guyon P M, Houver J C, Lebech M, Raseev G and Doweck D 2002 *Phys. Rev. A* **65** 020702
- [12] Jin C, Le A-T, Zhao S-F, Lucchese R R and Lin C D 2010 *Phys. Rev. A* **81** 033421
- [13] Burke P G 1978 *J. Phys. Colloq.* **39** C4-27
- [14] Tennyson J 2010 *Phys. Rep.* **491** 29
- [15] Burke P G 2011 *R-Matrix Theory of Atomic, Collisions: Application to Atomic Molecular and Optical Processes* (Berlin: Springer)
- [16] Harvey A G, Brambila D S, Morales F and Smirnova O 2014 *J. Phys. B: At. Mol. Opt. Phys.* **47** 215005
- [17] Mašén Z, Benda J, Gorfinkiel J D, Harvey A G and Tennyson J 2020 *Comput. Phys. Commun.* **249** 107092
- [18] Semenov S K, Cherepkov N A, Fecher G H and Schönhense G 2000 *Phys. Rev. A* **61** 032704
- [19] Cherepkov N A, Semenov S K, Hikosaka Y, Ito K, Motoki S and Yagishita A 2000 *Phys. Rev. Lett.* **84** 250
- [20] Semenov S K and Cherepkov N A 2002 *Phys. Rev. A* **66** 022708
- [21] Semenov S K and Cherepkov N A 2003 *J. Phys. B: At. Mol. Opt. Phys.* **36** 1409
- [22] Semenov S K, Kuznetsov V V, Cherepkov N A, Bolognesi P, Feyer V, Lahmam-Bennani A, Staicu Casagrande M E and Avaldi L 2007 *Phys. Rev. A* **75** 032707
- [23] Argenti L et al 2012 *New J. Phys.* **14** 033012
- [24] Toffoli D and Decleva P 2012 *J. Chem. Phys.* **137** 134103
- [25] Stener M, Fronzoni G and Decleva P 2005 *J. Chem. Phys.* **122** 234301
- [26] Mizuno T, Adachi J, Miyauchi N, Kazama M, Stener M, Decleva P and Yagishita A 2012 *J. Chem. Phys.* **136** 074305

- [27] Stener M, Decleva P, Yamazaki M, Adachi J-i and Yagishita A 2011 *J. Chem. Phys.* **134** 184305
- [28] Stener M, Bolognesi P, Coreno M, O’Keeffe P, Feyer V, Fronzoni G, Decleva P, Avaldi L and Kivimäki A 2011 *J. Chem. Phys.* **134** 174311
- [29] Catone D, Stener M, Decleva P, Contini G, Zema N, Prospero T, Feyer V, Prince K C and Turchini S 2012 *Phys. Rev. Lett.* **108** 083001
- [30] Powis I 1995 *Chem. Phys.* **201** 189
- [31] Powis I 2000 *J. Chem. Phys.* **112** 301
- [32] Forbes R et al 2020 *J. Phys. B: At. Mol. Opt. Phys.* **53** 155101
- [33] Bishop D M 1967 *Adv. Quantum Chem.* **3** 25
- [34] Sukhorukov V L, Demekhin V F, Yavna V A, Petrov I D, Demekhina L A and Lavrentiev S A 1983 *Coord. Chem. (USSR)* **9** 158
- [35] Demekhin Ph V, Omel’yanenko D V, Lagutin B M, Sukhorukov V L, Werner L, Ehresmann A, Schartner K H and Schmoranzler H 2007 *Opt. Spektrosc.* **102** 318
- [36] Demekhin Ph V, Ehresmann A and Sukhorukov V L 2011 *J. Chem. Phys.* **134** 024113
- [37] Galitskiy S A, Artemyev A N, Jänkälä K, Lagutin B M and Demekhin Ph V 2015 *J. Chem. Phys.* **142** 034306
- [38] Gianturco F A, Lucchese R R, Sanna N and Talamo A 1994 A generalized single centre approach for treating electron scattering from polyatomic molecules *Electron Collisions with Molecules, Clusters, and Surfaces* ed H Ehrhardt and L A Morgan (New York: Plenum) pp 1–86
- [39] Amusia M Y 1990 *Atomic Photoeffect* (New York: Plenum)
- [40] Sukhorukov V L, Petrov I D, Lagutin B M, Ehresmann A, Schartner K-H and Schmoranzler H 2019 *Phys. Rep.* **786** 1
- [41] Amusia M Y, Ivanov V K, Cherepkov N A and Chernysheva L V 1972 *Phys. Lett. A* **40** 361
- [42] Amus’ya M Y, Ivanov V K, Cherepkov N A and Chernysheva L V 1974 *Zh. Eksp. Teor. Fiz.* **66** 1537 http://www.jetp.ras.ru/cgi-bin/dn/e_039_05_0752.pdf
- [43] Tan K H and Brion C E 1978 *J. Electron Spectrosc. Relat. Phenom.* **13** 77
- [44] Houlgate R G, West J B, Codling K and Marr G V 1976 *J. Electron Spectrosc. Relat. Phenom.* **9** 205
- [45] Adam M Y, Wuilleumier F, Sandner N, Krummacher S, Schmidt V and Mehlhorn W 1978 *Japan. J. Appl. Phys.* **17** 170
- [46] Adam M Y, Morin P and Wendin G 1985 *Phys. Rev. A* **31** 1426
- [47] Lagutin B M et al 1999 *J. Phys. B: At. Mol. Opt. Phys.* **32** 1795
- [48] Adam M Y 1986 *Chem. Phys. Lett.* **128** 280
- [49] Lavrentiev S V, Vasil’eva M E, Petrov I D and Sukhorukov V L 1990 *Opt. Spektrosc.* **69** 307
- [50] Cacelli I, Carravetta V and Moccia R 1986 *Mol. Phys.* **59** 385
- [51] Johnson W R and Cheng K T 1979 *Phys. Rev. A* **20** 978
- [52] Huang K-N, Johnson W R and Cheng K T 1981 *At. Data Nucl. Data Tables* **26** 33
- [53] Lin C D 1974 *Phys. Rev. A* **9** 171
- [54] Starace A F 1982 Theory of atomic photoionization *Handbuch der Physik* vol 31 (Berlin: Springer) pp 1–121
- [55] Sorensen S L, Åberg T, Tulkki J, Rachlew-Källne E, Sundström G and Kirm M 1994 *Phys. Rev. A* **50** 1218
- [56] Saha H P 1989 *Phys. Rev. A* **39** 2456
- [57] Tulkki J, Åberg T, Mäntykenttä A and Aksela H 1992 *Phys. Rev. A* **46** 1357
- [58] Tulkki J 1993 *Phys. Rev. A* **48** 2048
- [59] Sukhorukov V L, Lavrentiev S V, Demekhin V F and Petrov I D 1984 *Khim. Fiz. (Sov.)* **3** 359
- [60] Lavrentiev S V, Lagutin B M, Vasil’eva M E and Sukhorukov V L 1988 *Khim. Fiz. (Sov.)* **7** 187
- [61] Lagutin B M, Sukhorukov V L and Demekhin V F 1989 *Chem. Phys. Lett.* **160** 432
- [62] Lagutin B M and Migal Y F 1989 *Teor. Eksp. Khim. (Sov.)* **25** 12
- [63] Lavrentiev S V, Petrov I D, Lagutin B M and Sukhorukov V L 1990 *Khim. Fiz. (Sov.)* **9** 81
- [64] Yavna V A, Nadolinskii A M and Demekhin V F 1990 *Opt. Spektrosc.* **69** 756
- [65] Lucchese R R and McKoy V 1981 *Phys. Rev. A* **24** 770
- [66] Lucchese R R, Raseev G and McKoy V 1982 *Phys. Rev. A* **25** 2572
- [67] Gianturco F A, Lucchese R R and Sanna N 1994 *J. Chem. Phys.* **100** 6464
- [68] Stratmann R E and Lucchese R R 1995 *J. Chem. Phys.* **102** 8493
- [69] Stratmann R E, Zuurales R W and Lucchese R R 1996 *J. Chem. Phys.* **104** 8989
- [70] Natalense A P P and Lucchese R R 1999 *J. Chem. Phys.* **111** 5344
- [71] Smith K, Henry R J W and Burke P G 1966 *Phys. Rev.* **147** 21
- [72] Burke P G and Seaton M J 1971 *Atomic and Molecular Scattering, Methods in Computational Physics* vol 10 (London: Academic) pp 1–80
- [73] Artemyev A N, Müller A D, Hochstuhl D and Demekhin Ph V 2015 *J. Chem. Phys.* **142** 244105
- [74] Müller A D, Artemyev A N and Demekhin Ph V 2018 *J. Chem. Phys.* **148** 214307
- [75] Müller A D, Kutscher E, Artemyev A N and Demekhin Ph V 2020 *J. Chem. Phys.* **152** 044302
- [76] Demekhin Ph V, Petrov I D, Sukhorukov V L, Kielich W, Reiss P, Hentges R, Haar I, Schmoranzler H and Ehresmann A 2010 *Phys. Rev. A* **80** 063425
- Demekhin Ph V, Petrov I D, Sukhorukov V L, Kielich W, Reiss P, Hentges R, Haar I, Schmoranzler H and Ehresmann A 2010 *Phys. Rev. A* **81** 069902(E) (erratum)
- [77] Demekhin Ph V, Petrov I D, Tanaka T, Hoshino M, Tanaka H, Ueda K, Kielich W and Ehresmann A 2010 *J. Phys. B: At. Mol. Opt. Phys.* **43** 065102
- [78] Demekhin Ph V, Petrov I D, Sukhorukov V L, Kielich W, Knie A, Schmoranzler H and Ehresmann A 2010 *Phys. Rev. Lett.* **104** 243001
- [79] Demekhin Ph V, Petrov I D, Sukhorukov V L, Kielich W, Knie A, Schmoranzler H and Ehresmann A 2010 *J. Phys. B: At. Mol. Opt. Phys.* **43** 165103
- [80] Demekhin Ph V, Lagutin B M and Petrov I D 2012 *Phys. Rev. A* **85** 023416
- [81] Knie A et al 2014 *Phys. Rev. A* **90** 013416
- [82] Antonsson E, Patanen M, Nicolas C, Benkoula S, Neville J J, Sukhorukov V L, Bozek J D, Demekhin Ph V and Miron C 2015 *Phys. Rev. A* **92** 042506
- [83] Knie A, Patanen M, Hans A, Petrov I D, Bozek J D, Ehresmann A and Demekhin Ph V 2016 *Phys. Rev. Lett.* **116** 193002
- [84] Nandi S, Nicolas C, Artemyev A N, Novikovskiy N M, Miron C, Bozek J D and Demekhin Ph V 2017 *Phys. Rev. A* **96** 052501
- [85] Ilchen M et al 2017 *Phys. Rev. A* **95** 053423
- [86] Novikovskiy N M, Sukhorukov V L, Artemyev A N and Demekhin Ph V 2019 *Eur. Phys. J. D* **73** 79
- [87] Hartmann G et al 2019 *Phys. Rev. Lett.* **123** 043202
- [88] Sann H et al 2016 *Phys. Rev. Lett.* **117** 263001
- [89] Tia M et al 2017 *Phys. Chem. Lett.* **8** 2780
- [90] Mhamdi A et al 2018 *Phys. Rev. Lett.* **121** 243002
- [91] Kircher M et al 2019 *Phys. Rev. Lett.* **123** 243201
- [92] Pier A et al 2020 *Phys. Rev. Res.* **2** 033209
- [93] Mhamdi A, Rist J, Havermeier T, Dörner R, Jahnke T and Demekhin Ph V 2020 *Phys. Rev. A* **101** 023404
- [94] Kaiser L et al 2020 *J. Phys. B: At. Mol. Opt. Phys.* **53** 194002
- [95] Kastirke G et al 2020 *Phys. Rev. X* **10** 021052
- [96] Kastirke G et al 2020 *Phys. Rev. Lett.* **125** 163201
- [97] Nalin G et al 2021 *Phys. Chem. Chem. Phys.* **23** 17248

- [98] Fehre K *et al* 2021 *Phys. Rev. Lett.* **127** 103201
- [99] Fehre K *et al* 2021 (arXiv:2101.03375)
- [100] Rist J *et al* 2021 *Nat. Commun.* **12** 6657
- [101] Hergenbahn U, Kugeler O, Rüdell A, Rennie E E and Bradshaw A M 2001 *J. Phys. Chem. A* **105** 5704
- [102] Lin P and Lucchese R R 2002 *J. Chem. Phys.* **117** 4348
- [103] Stener M, Fronzoni G and Decleva P 2002 *Chem. Phys. Lett.* **351** 469
- [104] Semenov S K *et al* 2006 *J. Phys. B: At. Mol. Opt. Phys.* **39** 375
- [105] Shigemasa E, Ueda K, Sato Y, Sasaki T and Yagishita A 1992 *Phys. Rev. A* **45** 2915
- [106] Burgess A 1963 *Proc. Phys. Soc.* **81** 442